

Performance of Ultra-Wideband Communications in the Presence of Interference

Li Zhao, *Student Member, IEEE*, and Alexander M. Haimovich, *Senior Member, IEEE*

Abstract—In this paper, we analyze the performance of ultra-wideband (UWB) communications in the presence of interference. Closed-form expressions are provided for the jam resistance of UWB with binary pulse position modulation utilizing rectangular pulses. A simple approximation is obtained for the special case of tone interference. The jam resistance analysis is extended to more practical UWB waveforms such as Gaussian and Rayleigh monocycles. A comparison between the interference suppression capabilities of UWB and direct-sequence spread-spectrum (DS-SS) is carried out under conditions similar to both systems. It is shown that in most cases, the jam suppression of UWB is superior to that of DS-SS.

Index Terms—Interference suppression, jam resistance, ultra-wideband communications (UWB).

I. INTRODUCTION

RECENT advancements in wireless communications generated a renewed interest in ultra-wideband (UWB) techniques [or as they are alternatively referred to—*impulse radio* (IR)] for communications applications. Unlike conventional wireless communications systems that are carrier-based, UWB-based communications is baseband. It uses a series of short pulses that spread the energy of the signal from near DC to a few gigahertz. One typical technique is to assign a window in time and shift the position of the pulse within that window. This is classical pulse position modulation (PPM). The increased interest in UWB communications is motivated by the assessment that this technology can provide high data rate communications. Very low power spectral densities and high processing gain will enable overlay and ensure only minimal mutual interference between UWB and other applications. The ultra-wide bandwidth makes communications robust with respect to multipath fading [1]–[3]. High ratio between the signal and information bandwidth (processing gain) makes this technology attractive to multiple access applications [1], [4], [5].

Since gigahertz unoccupied slices of bandwidth are not available at microwave frequencies, under FCC regulations UWB radio must be treated as spurious interference to all other communication systems. In addition, UWB radios operating over the densely populated frequency range below a few gigahertz,

must contend with a variety of interfering signals. These important requirements hint to similarities between UWB and more familiar spread-spectrum (SS) technologies, such as direct-sequence (DS). In this paper, we are concerned with analyzing jam resistance properties of UWB systems and comparing them to those of direct-sequence spread-spectrum (DS-SS). Jam resistance is provided by the SS processing gain and it is defined as the power advantage the jammer may have without disrupting communications.

The processing gains of UWB and DS-SS systems are obtained as a result of different underlying filtering operations. With traditional DS-SS, the bandwidth is spread by modulating the data message with a pseudo noise (PN) sequence. The detected output signal-to-noise ratio (SNR) is improved by the spreading ratio, which is the ratio of bandwidths of the SS and the information. This processing gain is equal to the spreading ratio and it is due to the noise-like PN property and the short duration of the chips modulating the information sequence. Unlike DS-SS, the spread bandwidth of the UWB waveform is generated directly and not by modulation with a separate spreading sequence. Thus, UWB is essentially a time-domain concept. The processing gain of UWB is due to the extremely short pulse, which generates a very wide instantaneous bandwidth signal, and is achieved at the receiver by time-gating matched to the pulse duration. This time gating reduces the power of a continuous-time waveform interference to the duty cycle of the UWB waveform. Traditional DS-SS has a constant envelope with a 100% duty cycle and a peak power P_{peak} equal to the average power P_{av} . With UWB, the pulse duration is extremely short with respect to the pulse repetition time resulting in pulse peak power hundreds of times larger than the average power. To compare the performance of UWB and DS-SS, we will assume that they have the same average power P_{av} (average power constraint), the same information sequence bit interval T_b and that both are subject to an interference with average power P_J . Performance is assumed interference limited, hence, the effect of additive white Gaussian noise (AWGN) is neglected.

This paper is organized as follows. Section II introduces the signal model including various UWB waveforms and their properties. The UWB performance analysis is developed in Section III. Comparison with DS-SS is carried out in Section IV. Finally, conclusions are provided in Section V.

II. SIGNAL MODEL

A. UWB Waveforms

UWB emissions are constrained by FCC regulation 47 CFR Section 15.5(d), which states that “Intentional radiators that

Manuscript received December 6, 2001; revised July 26, 2002. This work was supported in part by NSF Award number CCR 0085846 and in part by the New Jersey Center for Wireless Telecommunications. This paper was presented in part at the IEEE International Conference on Communications (ICC’01), Helsinki, Finland, June 11–15, 2001.

L. Zhao and A. M. Haimovich are with the Department of Electrical and Computer Engineering, New Jersey Institute of Technology, Newark, NJ 07102 USA (e-mail: lxz0111@oak.njit.edu; haimovic@njit.edu).

Digital Object Identifier 10.1109/JSAC.2002.805061

produce class B emissions (damped wave) are prohibited.” Various nondamped waveforms have been proposed for IR including Gaussian [4], Rayleigh, Laplacian, and cubic monocycles [6]. In general, the goal is to obtain a flat frequency spectrum of the transmitted signal over the bandwidth of the pulse and to avoid a DC component. In this paper, we first address the jam resistance properties of a UWB system with a rectangular pulse waveform. A rectangular pulse is not best suited for UWB applications, but is considered in this study since it enables to obtain closed-form expressions of the performance analysis. Such analysis is important since it provides insight into the mechanisms affecting the performance of UWB. More practical waveforms can be grouped in two categories according to their time symmetry. Gaussian and Laplacian monocycles have even symmetry, while Rayleigh and cubic monocycles have odd symmetry. In this paper, in addition to the rectangular waveform, we will study UWB utilizing Gaussian and Rayleigh monocycles. Performance of the latter entails complex mathematical formats that are difficult to reduce to closed-forms, hence, we rely mainly on computer-aided numerical analysis.

For a rectangular pulse $p_\rho(t)$ with pulsewidth T_p , we have

$$p_\rho(t) = \sqrt{\frac{1}{T_p}}, \quad 0 < t < T_p. \quad (1)$$

Comparing with a rectangular waveform, the principal characteristic of monocycle signals is that they have zero DC content to allow them to radiate effectively. The time domain representation of the Gaussian monocycle, $p_G(t)$, is [6]

$$p_G(t) = A_G \left[1 - \left(\frac{t}{\sigma} - 3.5 \right)^2 \right] \exp \left[-0.5 \left(\frac{t}{\sigma} - 3.5 \right)^2 \right] \quad (2)$$

where the relation between the pulsewidth T_p and the parameter σ is chosen $T_p = 7\sigma$. This pulsewidth contains 99.99% of the total energy in the Gaussian monocycle. The Rayleigh monocycle $p_R(t)$ is given by

$$p_R(t) = A_R \left[\frac{t - 3.5\sigma}{\sigma^2} \right] \exp \left[-0.5 \left(\frac{t}{\sigma} - 3.5 \right)^2 \right]. \quad (3)$$

The amplitudes A_G and A_R are chosen such that each monocycle has unit energy. Fig. 1 shows the monocycles with pulsewidth $T_p = 1$ ns.

The frequency spectra of the Gaussian and Rayleigh monocycles are given, respectively, by [6]:

$$S_G(f) = A_G \sqrt{2\pi\sigma^2} (2\pi\sigma f)^2 \exp \left[-\frac{(2\pi\sigma f)^2}{2} \right] \quad (4)$$

and

$$S_R(f) = A_R \sqrt{2\pi} (2\pi\sigma f) \exp \left[-\frac{(2\pi\sigma f)^2}{2} \right]. \quad (5)$$

The effective bandwidth is defined as $W = f_H - f_L$, where f_H and f_L are the frequencies measured at the -3 dB emission points. A numerical evaluation according to this definition, shows that the Gaussian and Rayleigh monocycles have the same effective bandwidths [6]

$$W_G = W_R = 0.1853/\sigma. \quad (6)$$

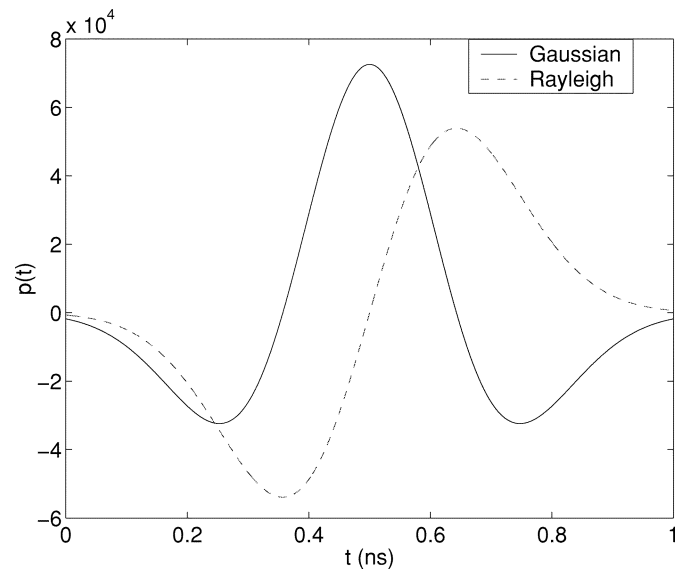


Fig. 1. UWB monocycles with $T_p = 1$ ns.

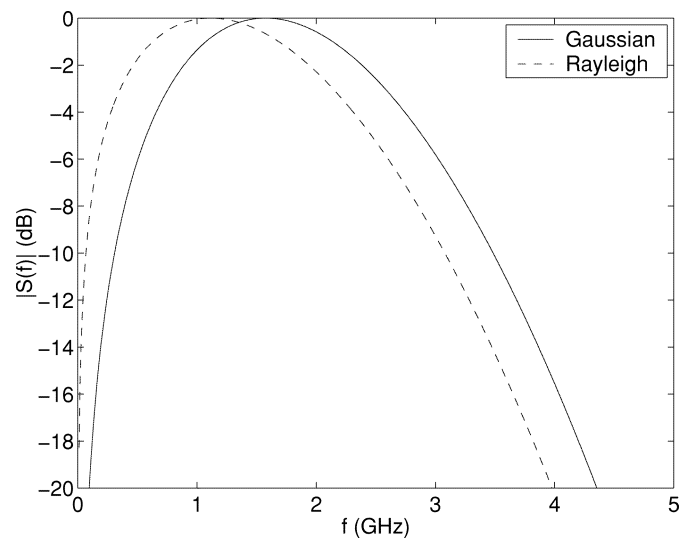


Fig. 2. Frequency spectrum of UWB monocycles.

Since pulsewidth $T_p = 7\sigma$, the bandwidths W_G and W_R are related to T_p as following:

$$W_G = W_R = \frac{c}{T_p} \quad (7)$$

where $c = 1.2971$. Fig. 2 shows the frequency spectrums of monocycles with pulse duration $T_p = 1$ ns.

B. Signal Model

Consider a single-user UWB pulse position modulated and time-hopping communication system. The time-hopping binary PPM signal of a single user can be written [4]

$$G(t) = \sum_{k=-\infty}^{+\infty} \sqrt{E_p} p(t - kT_f - c_k T_c - d_{[k/N_p]}) \delta \quad (8)$$

where $p(t)$ is the UWB pulse, E_p is the energy per pulse, T_f is the pulse repetition time interval, the sequence c_k represents the time hopping, with $c_k T_c$ an additional time shift to the

k th pulse of the communication burst. For a fixed T_f , the information sequence bit rate $R_b = 1/(N_p T_f)$ determines N_p , the number of pulses that are modulated by a given binary symbol. The information binary sequence $d_{[k/N_p]} \in \{0, 1\}$ changes at multiples of N_p . The parameter δ is the pulse position offset when $d_{[k/N_p]} = 1$.

The optimal receiver for a single user using UWB communications as defined so far, is a pulse correlation receiver. The template waveform used in the correlation receiver is given by

$$V(t) = p(t) - p(t - \delta). \quad (9)$$

For a received signal

$$Y(t) = G(t) + J(t) \quad (10)$$

where $J(t)$ is the interference waveform, the correlation receiver computes the decision statistic

$$D_q = \sum_{k=0}^{N_p-1} \int_{\tau+kT_f}^{\tau+(k+1)T_f} Y(t)V(t - kT_f - c_k T_c - \tau) \quad (11)$$

where τ represents the delay with respect to the time origin and $q = [j/N_p]$. Note that we assume perfect synchronization (known τ). Decisions are made according to

$$d_q = \begin{cases} 0, & \text{if } D_q \geq 0 \\ 1, & \text{if } D_q \leq 0 \end{cases}. \quad (12)$$

To simplify the theoretical analysis of jam resistance performance, we make the following additional assumptions:

- 1) No time-hopping code is used, i.e., $c_k = 0$.
- 2) To derive the performance of UWB in the presence of interference, we assume 2-PPM symbols. The pulse position time shift for data "0" equals the pulsewidth, i.e., $\delta = T_p$. Thus, the two PPM symbols are $s_1(t) = p(t)$ and $s_2(t) = p(t - T_p)$.
- 3) The parameter N_p is the number of UWB pulses transmitted for each data symbol. System performance is a function of the signal-to-interference ratio (SIR) per bit E_b/J_0 , where $E_b = N_p E_p$ and J_0 is the interference power spectral density. The average power of the transmitted signal needs to be consistent with FCC regulations. For a given scenario (distance, pulse interval T_f , pulsewidth T_p), E_b is determined by the FCC constraint. For highest capacity $N_p = 1$. Alternatively, at the expense of capacity, $N_p > 1$ can be used to reduce the transmitted peak power. For simplicity, and without loss of generality, we assume that for each data symbol, a single UWB pulse is transmitted ($N_p = 1$). This assumption implies the information bit interval equals the UWB pulse interval, $T_b = T_f$.
- 4) The interference $J(t)$ is assumed a passband signal with carrier frequency f_J . It is modeled as a continuous-time wide sense stationary zero-mean random process with bandwidth W_J and power spectral density (see Fig. 3)

$$S_J(f) = \begin{cases} \frac{J_0}{2}, & |f - f_J| \leq W_J \\ 0, & \text{otherwise} \end{cases}. \quad (13)$$

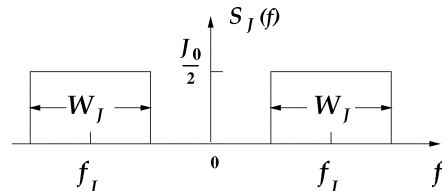


Fig. 3. Power spectral density of interference $J(t)$.

It follows that the time autocorrelation $R_J(\tau)$ of the interference is:

$$R_J(\tau) = J_0 \frac{\sin \pi W_J \tau}{\pi \tau} \cos 2\pi f_J \tau. \quad (14)$$

- 5) System performance is assumed interference limited. The effect of thermal noise is neglected.

With those assumptions, the signal received over a bit interval $kT_b \leq t \leq (k+1)T_b$, ($-\infty < k < +\infty$), is given by

$$Y_k(t) = \sqrt{E_p} p(t - kT_f - dT_p) + J(t) \quad (15)$$

where $d \in \{0, 1\}$ is the information bit.

Since by assumption $\int_0^{T_f} p(t)^2 dt = 1$, the cross correlation $\int_0^{T_f} p(t - dT_p)V(t) dt$ over the pulse interval T_f between the UWB pulse and the template at the receiver is 1 for $d = 1$ and -1 for $d = 0$. Hence, the correlator output corresponding to an information bit is given by:

$$\begin{aligned} y(kT_b) &= \int_{kT_b}^{(k+1)T_b} Y_k(t)V(t - kT_f) dt \\ &= \pm \sqrt{E_p} + j(kT_b) \end{aligned} \quad (16)$$

where $\pm \sqrt{E_p}$ corresponds to the transmitted information bit "1" and "0," respectively, and $j(kT_b)$ represents the interference component.

The interference component at the output of the correlator can be expressed

$$\begin{aligned} j(kT_b) &= \int_{kT_b}^{(k+1)T_b} J(t)V(t - kT_f) dt \\ &= \int_0^{T_f} J(t + kT_f)V(t) dt. \end{aligned} \quad (17)$$

The *processing gain* is defined as the ratio of the output to the input SIR

$$PG = \frac{\text{SIR}_{\text{out}}}{\text{SIR}_{\text{in}}}. \quad (18)$$

The *jam resistance* JR is defined as the margin that the processing gain provides above the minimum SIR, SIR_D , required to meet system performance specs

$$JR = PG - \text{SIR}_D. \quad (19)$$

Let the average power of the interference waveform $J(t)$ at the receiver input be P_J , and the average signal power be P_s . The average signal power can be expressed $P_s = E_p/T_b$. Then, the input SIR is given by

$$\text{SIR}_{\text{in}} = \frac{E_p}{T_b P_J}. \quad (20)$$

From (16), the signal power at the output of the correlator is given by E_p . The interference power at the output depends on the statistical characteristics of the interference and on the UWB pulse

$$\text{SIR}_{\text{out}} = \frac{E_p}{E[j^2(kT_b)]}. \quad (21)$$

From (18) and (20), (21), the processing gain is given by

$$\text{PG} = \frac{T_b P_J}{E[j^2(kT_b)]}. \quad (22)$$

The interference $J(t)$ is modeled by a random process, hence, the functionals $j(kT_b)$ defined in (17) are random variables. Since interference is assumed zero-mean and wide-sense stationary, its power at the correlator output is expressed

$$\begin{aligned} E[j^2(kT_b)] &= E \left[\int_0^{T_f} J(t_1 + kT_f) V(t_1) dt, \right. \\ &\quad \left. \times \int_0^{T_f} J(t_2 + kT_f) V(t_2) dt_2 \right] \\ &= \int_0^{T_f} \int_0^{T_f} R_J(t_1 - t_2) V(t_1) V(t_2) dt_1 dt_2. \end{aligned} \quad (23)$$

III. PERFORMANCE ANALYSIS

A. Jam Resistance With Rectangular Pulses

The mathematical model of the rectangular pulse $p_\rho(t)$ is given in (1). At the receiver, the template for $p_\rho(t)$ is

$$V_\rho(t) = \begin{cases} \sqrt{\frac{1}{T_p}} & 0 < t < T_p \\ -\sqrt{\frac{1}{T_p}} & T_p < t < 2T_p \end{cases}. \quad (24)$$

Using (24) in (23), the time autocorrelation of the interference samples can be expressed

$$\begin{aligned} E[j^2(kT_b)] &= \frac{1}{T_p} \int_0^{T_p} \int_0^{T_p} R_J(t_1 - t_2) dt_1 dt_2 \\ &\quad + \frac{1}{T_p} \int_{T_p}^{2T_p} \int_{T_p}^{2T_p} R_J(t_1 - t_2) dt_1 dt_2 \\ &\quad - \frac{1}{T_p} \int_0^{T_p} \int_{T_p}^{2T_p} R_J(t_1 - t_2) dt_1 dt_2 \\ &\quad - \frac{1}{T_p} \int_{T_p}^{2T_p} \int_0^{T_p} R_J(t_1 - t_2) dt_1 dt_2. \end{aligned}$$

Set $t_1 - t_2 = \tau$. Since the interference is assumed wide sense stationary, $R_J(\tau) = E[J(t)J(t - \tau)]$ and $E[j^2(kT_b)]$ can be reduced to the single integral

$$E[j^2(kT_b)] = \int_{-T_p}^{T_p} \left(1 - \frac{|\tau|}{T_p} \right) [2R_J(\tau) - R_J(\tau + T_p) - R_J(\tau - T_p)] d\tau. \quad (25)$$

Define the parameters $\alpha = T_p W_J$, $x = W_J \tau$, $\beta = T_f/T_p$, and $\gamma = f_J T_p$. Note that α is the interference time-bandwidth product over the duration of the pulse, $\beta = T_f/T_p$ is the UWB spreading ratio, and γ is number of cycles of the interference

carrier frequency during an UWB pulse. Substitute $R_J(\tau)$ from (14) in (25). After some algebraic manipulations, (25) can be expressed

$$E[j^2(kT_b)] = J_0 \Phi(\alpha, \gamma) \quad (26)$$

where

$$\Phi(\alpha, \gamma) = 2\Phi_0(\alpha, \gamma) - \Phi_1(\alpha, \gamma) - \Phi_2(\alpha, \gamma). \quad (27)$$

The quantities $\Phi_0(\alpha, \gamma)$, $\Phi_1(\alpha, \gamma)$, and $\Phi_2(\alpha, \gamma)$ are defined, respectively

$$\Phi_0(\alpha, \gamma) = \int_{-\alpha}^{\alpha} \left(1 - \frac{|x|}{\alpha} \right) \frac{\sin \pi x}{\pi x} \cos 2\pi \frac{\gamma}{\alpha} x dx \quad (28)$$

$$\Phi_1(\alpha, \gamma) = \int_{-\alpha}^{\alpha} \left(1 - \frac{|x|}{\alpha} \right) \frac{\sin \pi(x + \alpha)}{\pi(x + \alpha)} \cos 2\pi \frac{\gamma}{\alpha} (x + \alpha) dx \quad (29)$$

and

$$\Phi_2(\alpha, \gamma) = \int_{-\alpha}^{\alpha} \left(1 - \frac{|x|}{\alpha} \right) \frac{\sin \pi(x - \alpha)}{\pi(x - \alpha)} \cos 2\pi \frac{\gamma}{\alpha} (x - \alpha) dx. \quad (30)$$

From (21) and (23), the output SIR is then given by

$$\text{SIR}_{\text{out}} = \frac{E_p}{J_0 \Phi(\alpha, \gamma)}. \quad (31)$$

Since $E_p = P_s T_b$, $J_0 = P_J/W_J$, $T_b W_J = (T_p W_J)(T_b/T_p) = \alpha\beta$, we finally have

$$\text{SIR}_{\text{out}} = \frac{P_s}{P_J} \frac{\alpha\beta}{\Phi(\alpha, \gamma)} = \text{SIR}_{\text{in}} \frac{\alpha\beta}{\Phi(\alpha, \gamma)}. \quad (32)$$

The processing gain of UWB with a rectangular pulse is then given by

$$\text{PG}_\rho = \frac{\alpha\beta}{\Phi(\alpha, \gamma)}. \quad (33)$$

Let us discuss further the physical meaning of the parameters α , β , and γ in (33).

- 1) The parameter $\alpha = W_J T_p$, serves as a measure of the ratio of the interference and the UWB bandwidths. Specifically, $\alpha \rightarrow 1$ corresponds to an interference bandwidth commensurate with that of the UWB signal, and $\alpha \rightarrow 0$ represents a narrowband interference. The latter is the case greater practical interest.
- 2) The variable $\beta = T_f/T_p$ is the spreading ratio of UWB signals. Typical values of β are greater than 100. The corresponding duty cycle of UWB pulses is less than 1%.
- 3) The parameter $\gamma = f_J T_p$ measures the number of jammer carrier cycles during the UWB pulse. Since we consider only inband interference, $0 \leq \gamma \leq 1$.

When the interference is narrowband such that $\alpha \rightarrow 0$, we have the following approximations:

$$\Phi_0(\alpha \rightarrow 0, \gamma) = \int_{-\alpha}^{\alpha} \left(1 - \frac{|x|}{\alpha} \right) \cos 2\pi \frac{\gamma}{\alpha} x dx \quad (34)$$

$$\Phi_1(\alpha \rightarrow 0, \gamma) = \int_{-\alpha}^{\alpha} \left(1 - \frac{|x|}{\alpha} \right) \cos 2\pi \frac{\gamma}{\alpha} (x + \alpha) dx \quad (35)$$

$$\Phi_2(\alpha \rightarrow 0, \gamma) = \int_{-\alpha}^{\alpha} \left(1 - \frac{|x|}{\alpha} \right) \cos 2\pi \frac{\gamma}{\alpha} (x - \alpha) dx. \quad (36)$$

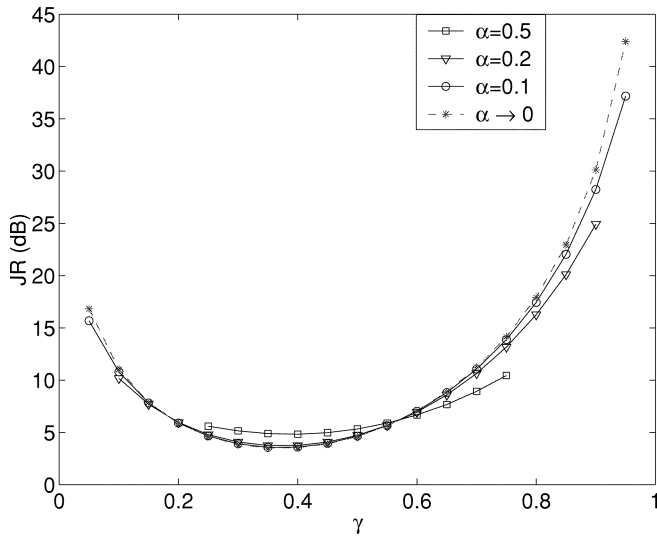


Fig. 4. Jam resistance of UWB utilizing rectangular pulses with different α .

Combining these result in (27), we have $\Phi(\alpha \rightarrow 0, \gamma)$

$$\Phi(\alpha \rightarrow 0, \gamma) = \frac{\alpha}{(\pi\gamma)^2} (1 - \cos 2\pi\gamma)^2. \quad (37)$$

From (33), when $\alpha \rightarrow 0$ the processing gain for a rectangular pulse is

$$PG_p(\alpha \rightarrow 0) = \frac{\beta(\pi\gamma)^2}{(1 - \cos 2\pi\gamma)^2}. \quad (38)$$

To evaluate the jam resistance JR_p (defined in (19)) of an UWB system with a rectangular pulse, we assumed that the required system performance is a bit error probability of $P_b = 10^{-6}$. For 2-PPM, the corresponding $SIR_D = 13$ dB, hence, the jam resistance $JR_p = PG_p - 13$ (dB).

Fig. 4 illustrates the relationship between the jam resistance and parameter γ for UWB with a rectangular pulse and spreading ratio $\beta = 100$. Various cases of interference are shown (parameterized by α). The curves in the figure (except the one labeled $\alpha \rightarrow 0$) were generated using (33). The curve for $\alpha \rightarrow 0$ was generated using (38). It is observed that the jam resistance approaches its minimum value when γ is in the neighborhood of 0.4 (corresponding to an interference carrier of $f_J = 0.4/T_p$). Also, shown in the figure is the case of wideband interference, $\alpha = 0.5$. In this case, the largest $\gamma = f_J T_p$ shown is 0.75, such that the full range of the interference bandwidth is still contained within the UWB bandwidth. In the wideband case, the jam resistance is seen to hover around the level of 7 dB (corresponding to β dB $-\text{SNR}_D = 20 - 13$ dB).

Some understanding of the mechanism of interference suppression in UWB PPM communications can be gained from (14) and (25). The interference power in (25) is reduced through time gating over the interval of $2T_p$. This is the processing gain associated with the spreading-despreading operation. An additional interference suppression mechanism is obtained through the subtraction of time-shifted autocorrelation functions. From (14), it is observed that the autocorrelation of the interference takes on positive and negative values as a function of the time lag τ . From (25), the interference power is computed from subtracting values of the interference autocorrelation function.

For a narrowband interference, the correlation is high, and the subtraction operation will, in general, entail an additional suppression of interference. For some values of the interference carrier, (25) results in enhanced interference (corresponding to subtracting a negative value of the autocorrelation function). For wideband interference $\alpha = 0.5$, this effect is diminished since the interference values become uncorrelated. Indeed, this is borne out by Fig. 4, where for $\alpha = 0.5$ the jam resistance is closer to the value predicted by the spreading ratio.

B. Jam Resistance With Monocycles

Two different monocycles are chosen for analysis, Gaussian and Rayleigh. Temporal and spectral characteristics of the monocycles are shown in Figs. 1 and 2, respectively. For binary PPM, the receiver correlates the received signal with the waveform $V(t) = p(t) - p(t - \delta)$, where the pulse $p(t)$ is the appropriate monocycle.

Our goal is to evaluate the jam resistance (19), or equivalently, the processing gain (22). Using (14) in (23), we get

$$E[j^2(kT_b)] = \int_0^{T_f} \int_0^{T_f} J_0 \frac{\sin \pi W_J \tau}{\pi \tau} \times \cos 2\pi f_J \tau V(t_1) V(t_2) dt_1 dt_2. \quad (39)$$

Set $W_J t_1 = t'_1$, $W_J t_2 = t'_2$, and recall the definitions $\alpha = T_p W_J$, $\beta = T_f / T_p$, and $\gamma = f_J T_p$. Then $E[j^2(kT_b)]$ can be expressed

$$E[j^2(kT_b)] = J_0 \Theta(\alpha, \gamma) \quad (40)$$

where $\Theta(\alpha, \gamma)$ is given by the expression

$$\Theta(\alpha, \gamma) = \int_0^{2\alpha} \int_0^{2\alpha} \frac{\sin \pi(t'_1 - t'_2)}{\pi(t'_1 - t'_2)} \cos 2\pi \frac{\gamma}{\alpha} (t'_1 - t'_2) V \times \left(\frac{t'_1}{W_J} \right) V \left(\frac{t'_2}{W_J} \right) dt'_1 dt'_2. \quad (41)$$

Since by assumption $E[J(t)] = 0$, clearly the mean value of the interference component at the output of the receiver $E[j(T_b)] = 0$. From (22) and (40), the UWB processing gain for monocycles is given by

$$PG = \frac{\alpha\beta}{\Theta(\alpha, \gamma)} \quad (42)$$

where $\Theta(\alpha, \gamma)$ is computed for either the Gaussian or Rayleigh monocycle.

Comparing the processing gain of monocycles in (42) with that of the rectangular pulse in (33), we observe that they have the same format except for the different factors Θ and Φ , which are determined by the specific pulse waveform.

Similar to the analysis for rectangular pulse, we chose a spreading ratio of $\beta = 100$ for computing the jam resistance of monocycles. In Fig. 5, jam resistance of three types of waveforms is plotted for an interference carrier with $0 < \gamma < 1$ and two values of the interference time-bandwidth product over the duration of the UWB pulse. Other than the case of $\gamma > 0.6$, the suppression ability of the monocycles significantly exceeds that of the rectangular pulse. For all waveforms, the curves for $\alpha = 10^{-1}$ almost overlap with those for $\alpha = 10^{-3}$. The Gaussian pulse provides the highest overall jam resistance. The

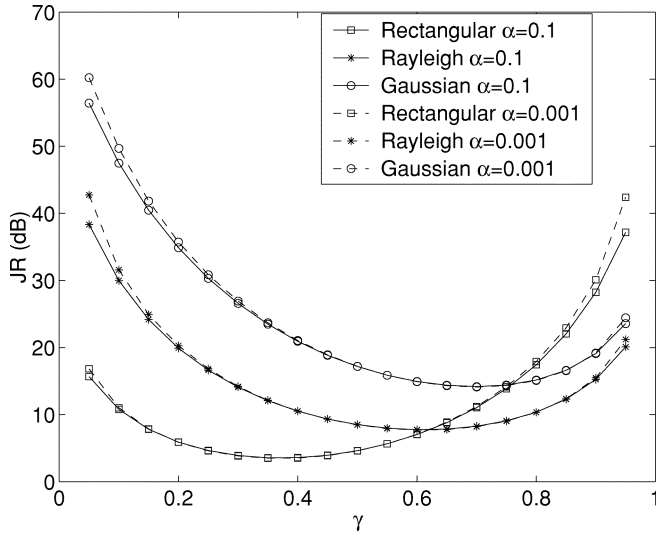


Fig. 5. Jam resistance for narrowband interference of UWB utilizing monocycles.

different performance of the Gaussian and Rayleigh pulses can be explained from the frequency domain characteristics of the pulses and interference. The performance evaluation in this paper is done with predominantly low frequency interference. From Fig. 2, it is obvious that the UWB Gaussian pulse matched filter will filter out more of the low frequency interference than the Rayleigh pulse matched filter.

IV. COMPARISON OF UWB AND DS-SS

Conventional DS-SS signals are similar in the sense that both use a short pulse (PN chip in DS-SS) to get the SS effect. But, there are fundamental differences between the two methods. The UWB waveform is carrier-less and it does not have a constant envelope. Conversely, DS-SS signals have a constant envelope with the information waveform being modulated by a SS waveform and a carrier frequency. Furthermore, in typical applications, the chip of DS-SS will have a much longer duration than the UWB pulsewidth. Hence, the same interference with a certain bandwidth W_J , could be narrowband with respect to UWB and wideband with respect to DS-SS. For UWB, the parameter α was defined as pulsewidth times interference bandwidth. This definition can be extended to DS-SS, where the pulsewidth is the chip time T_c . For DS-SS, $\alpha = T_c W_J$. Thus, α serves as a measure of comparative bandwidth between the interference and either system. It is of interest to compare the performance of the two systems in the presence of interference. Notably, the mechanisms for interference suppression are quite different. With DS-SS, the interference is typically spread by cross-correlation with the PN sequence and is subsequently reduced by lowpass filtering at the data bandwidth. In contrast, as explained at the end of the previous section, with UWB there are two mechanisms for interference suppression: 1) time windowing over the duration of the short UWB pulse and 2) the cross correlation at the receiver of the interference with the template (9) results in reduction of a narrowband interference due to the high correlation of the interference at times t and $t \pm T_p$.

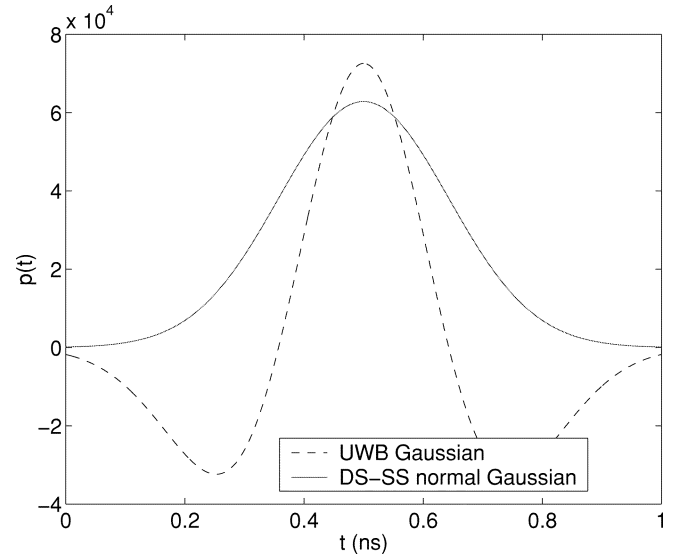


Fig. 6. Gaussian chip waveform of DS-SS and Gaussian monocycle.

A. Jam Resistance of DS-SS

To proceed with the comparison between UWB and DS-SS, consider a DS-SS system utilizing binary PSK, with a bit interval T_b , chip interval T_c , and spreading ratio $L_c = T_b/T_c$. Within the bit interval $0 \leq t \leq T_b$, the transmitted signal is [7]

$$S(t) = \sum_{n=0}^{L_c-1} d_0 \sqrt{\frac{2E_b}{T_b}} c_n p_c(t - nT_c) \cos 2\pi f_c t \quad (43)$$

where $d_0 = \pm 1$ is the information symbol, $c_n = \pm 1$ denotes the PN code sequence, $p_c(t)$ is the chip waveform, and E_c is the energy per chip. The energy per bit of the DS-SS is $E_b = L_c E_c/2$. The code chip sequence is assumed uncorrelated such that $E[c_n c_m] = E[c_n]E[c_m]$ for $n \neq m$.

For comparison with the UWB Gaussian monocycle, assume that the DS-SS chip waveform $p_c(t)$ is a normal Gaussian pulse as shown in Fig. 6 and given by

$$p_c(t) = A_c \exp \left[-0.5 \left(\frac{t}{\sigma} - 3.5 \right)^2 \right] \quad (44)$$

where σ is a chip width parameter. The amplitude A_c is chosen such that the pulse has unit energy.

The pulsewidth is chosen $T_c = 7\sigma$, ensuring that the time-limited pulse contains more than 99% of the energy of the Gaussian waveform defined in (44).

The Gaussian monocycle is the derivative of the Gaussian pulse. In practice, the monocycle is the transmitted waveform resulting from high-pass filtering by the transmit antenna of a Gaussian pulse. In Fig. 6, the temporal waveforms of the Gaussian normal and monocycle pulses are shown for the same time duration.

Similar to the model in (10), the received signal $Y(t)$ is corrupted by interference modeled by (13). Assuming ideal phase coherence and synchronization at the receiver, following carrier

demodulation with $\cos 2\pi f_c t$ and despreading with the PN sequence $\sum_{n=0}^{L_c-1} c_n p_c(t - jT_c)$, the output of the DS-SS receiver at the sampling instant $t = T_b$ is:

$$y(T_b) = \pm \frac{1}{2} L_c \sqrt{E_c} + j(T_b) \quad (45)$$

where $j(T_b)$ represents the interference component, which has the form

$$\begin{aligned} j(T_b) &= \int_0^{T_b} J(t) \sum_{n=0}^{L_c-1} c_n p_c(t - nT_c) \cos 2\pi f_c t dt \\ &= \sum_{n=0}^{L_c-1} c_n j_n \end{aligned} \quad (46)$$

where

$$j_n = \int_{nT_c}^{(n+1)T_c} J(t) p_c(t - nT_c) \cos 2\pi f_c t dt. \quad (47)$$

Since by assumption, the PN sequence has uncorrelated terms and $E[c_n^2] = 1$

$$E[j^2(T_b)] = L_c E[j_n^2]. \quad (48)$$

To evaluate the moment $E[j_n^2]$, we substitute $R_J(\tau)$ (14), into $E[j_n^2]$. By neglecting double frequency terms, we obtain the result

$$\begin{aligned} E[j_n^2] &= \frac{J_0}{4} \int_0^{T_c} \int_0^{T_c} p_c(t_1) p_c(t_2) \frac{\sin \pi W_J (t_1 - t_2)}{\pi (t_1 - t_2)} \\ &\quad \times \cos 2\pi (f_J - f_c) (t_1 - t_2) dt_1 dt_2. \end{aligned} \quad (49)$$

Set $W_J t_1 = t'_1$, $W_J t_2 = t'_2$, $W_J T_c = \alpha$, and $\Delta f = f_J - f_c$. Then, $E[j_n^2]$ can be expressed as follows:

$$\begin{aligned} E[j_n^2] &= \frac{J_0}{4} \int_0^\alpha \int_0^\alpha p_c\left(\frac{t'_1}{W_J}\right) p_c\left(\frac{t'_2}{W_J}\right) \frac{\sin \pi (t'_1 - t'_2)}{\pi (t'_1 - t'_2)} \\ &\quad \times \cos 2\pi \frac{\Delta f}{W_J} (t'_1 - t'_2) dt'_1 dt'_2. \end{aligned} \quad (50)$$

In (50), Δf denotes the interference carrier offset with respect to the DS-SS carrier. Define $\nu = \Delta f T_c$, then, ν measures the ratio of interference carrier to system bandwidth. Since there is assumed a passband prefilter with bandwidth W at the front end of the DS-SS receiver, for $-W/2 \leq \Delta f \leq W/2$, we have $-0.5 \leq \nu \leq 0.5$. Thus, (50) can be rewritten

$$\begin{aligned} E[j_n^2] &= \frac{J_0}{4} \int_0^\alpha \int_0^\alpha p_c\left(\frac{t'_1}{W_J}\right) p_c\left(\frac{t'_2}{W_J}\right) \frac{\sin \pi (t'_1 - t'_2)}{\pi (t'_1 - t'_2)} \\ &\quad \times \cos 2\pi \frac{\nu}{\alpha} (t'_1 - t'_2) dt'_1 dt'_2. \end{aligned} \quad (51)$$

Therefore, the SNR_{in} is

$$\text{SNR}_{\text{in}} = \frac{E_b}{E[j^2(T_b)]} = \frac{E_b}{L_c \frac{J_0}{4} I(\alpha, \nu)} \quad (52)$$

where $I(\alpha, \nu)$ is

$$\begin{aligned} I(\alpha, \nu) &= \int_0^\alpha \int_0^\alpha p_c\left(\frac{t'_1}{W_J}\right) p_c\left(\frac{t'_2}{W_J}\right) \frac{\sin \pi (t'_1 - t'_2)}{\pi (t'_1 - t'_2)} \\ &\quad \times \cos 2\pi \frac{\nu}{\alpha} (t'_1 - t'_2) dt'_1 dt'_2. \end{aligned} \quad (53)$$

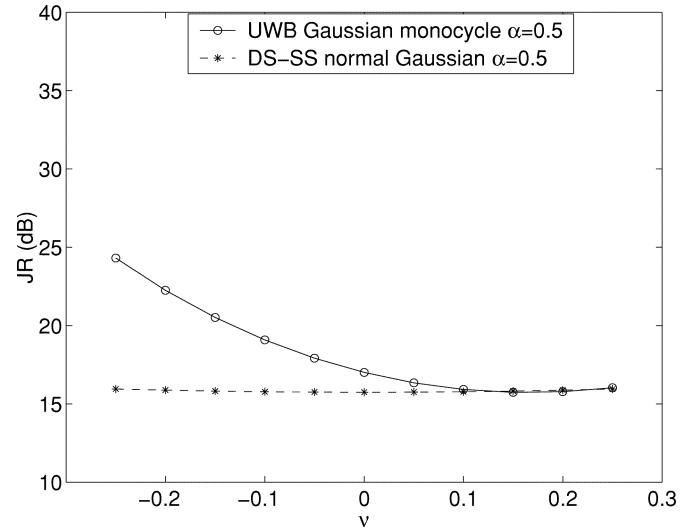


Fig. 7. Comparison between UWB and DS-SS for wideband interference $\alpha = 0.5$.

With the interference power spectral density $J_0 = P_J/W_J$ and the SS signal power $P_s = L_c E_c/2T_b$, we finally have

$$\text{SNR}_{\text{out}} = \frac{P_s}{P_J} \frac{2\alpha L_c}{I(\alpha, \nu)} = \text{SNR}_{\text{in}} \frac{2\alpha L_c}{I(\alpha, \nu)}. \quad (54)$$

It follows that the processing gain of DS-SS, PG is

$$\text{PG} = \frac{2\alpha L_c}{I(\alpha, \nu)}. \quad (55)$$

For a bit-error rate (BER) of 10^{-6} , the required SNR is $\text{SNR}_{\text{D}} = 10$ dB, hence, the jam resistance of DS-SS is given by

$$\text{JR} = \frac{2\alpha L_c}{I(\alpha, \nu)} - 10 \text{ (dB)}. \quad (56)$$

B. Comparison of UWB and DS-SS

Comparing the processing gains of UWB with a Gaussian monocycle (42) and DS-SS with Gaussian chips (55), it is observed that they have a similar form. Both processing gains are function of the parameter α . As mentioned earlier, the parameter α measures the comparative bandwidth between the interference and either system. Both parameters β and L_c have the same meaning of spreading ratio. The two processing gain expressions contain different parameters for the interference carrier offset. With UWB, this parameter is $\gamma = f_J T_p$, while with DS-SS it is $\nu = (f_J - f_c) T_c$. We can relate the two parameters as follows. Since UWB is carrier less, we define the "carrier" as the center frequency $W/2$ of UWB bandwidth. It follows that for UWB, the interference carrier offset is $\Delta f = f_J - W/2$. From the definition of γ , we have

$$\gamma = f_J T_p = \left(\Delta f + \frac{W}{2} \right) T_p = \nu + \frac{c}{2}. \quad (57)$$

Figs. 7 and 8 show the comparison of jam resistance with $-0.5 \leq \nu \leq 0.5$, for wideband interference ($\alpha = 0.5$) and narrowband interference ($\alpha \ll 1$), respectively. The two figures were generated with the same bandwidth spreading ratio for the both the UWB and DS-SS signals, i.e., $\beta = L_c = 100$. In

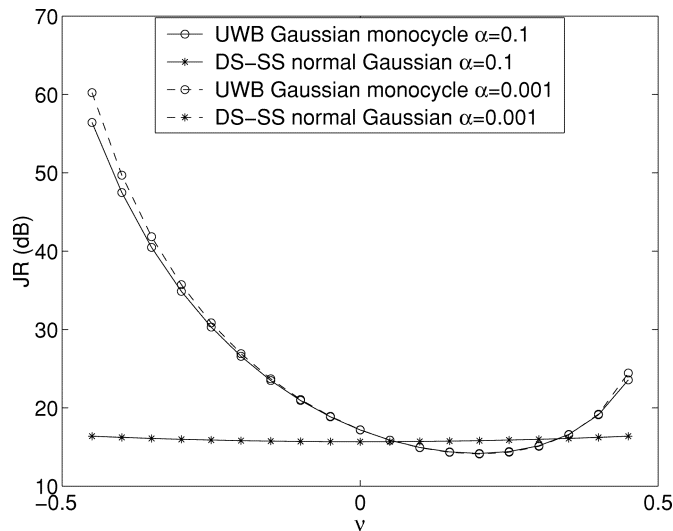


Fig. 8. Comparison between UWB and DS-SS for narrowband interference $\alpha \ll 1$.

Fig. 7, the wideband interference is wholly contained within the UWB bandwidth. It is observed that UWB has a higher jammer resistance than DS-SS for all values of ν . As for narrowband interference shown in Fig. 8, it is obvious that the UWB system have a higher ability to suppress interference than DS-SS for most cases of $-0.5 \leq \nu \leq 0.5$. Furthermore, the advantage of UWB increases dramatically when $\nu \rightarrow -0.5$ and $\nu \rightarrow 0.5$.

V. CONCLUSION

We analyzed the performance of UWB with binary PPM in the presence of interference. Closed-form expressions were provided for the jam resistance of a PPM UWB system utilizing rectangular pulses. A simple closed form approximation was obtained for the special case of narrowband interference. The analysis was then extended to two more practical UWB waveforms, namely Gaussian and Rayleigh monocycles. A comparison between the interference suppression capabilities of UWB and DS-SS was executed under certain assumptions. It was shown that for both narrowband and wideband interference, UWB has a significant advantage in interference suppression ability over DS-SS.

REFERENCES

[1] M. Z. Win, "Ultra-Wide Bandwidth Spread-Spectrum Techniques for Wireless Multiple-Access Communications," Ph.D. Thesis, Electrical Engineering, Univ. Southern California, Los Angeles, CA., Jan. 1998.

[2] M. Z. Win and R. A. Scholtz, "Impulse radio: How it works," *IEEE Commun. Lett.*, vol. 2, pp. 36–38, Feb. 1998.
 [3] R. J. Cramer, M. Z. Win, and R. A. Scholtz, "Evaluation of the multipath characteristics of the impulse radio channel," in *Proc. PIMRC'98*, vol. 2, 1998, pp. 864–868.
 [4] R. A. Scholtz, "Multiple access with time-hopping impulse modulation," *Proc. IEEE MILCOM'93*, vol. 2, pp. 447–450, Oct. 1993.
 [5] M. Z. Win and R. A. Scholtz, "Comparisons of analog and digital impulse radio for wireless multiple-access communications," in *Proc. IEEE ICC'97*, vol. 1, June 1997, pp. 91–95.
 [6] J. T. Conroy, J. L. LoCicero, and D. R. Ucci, "Communication techniques using monopulse waveforms," in *Proc. IEEE MILCOM'99*, vol. 2, 1999, pp. 1191–1185.
 [7] J. G. Proakis and M. Salehi, *Communication Systems Engineering*. Englewood Cliffs, NJ: Prentice-Hall, 1994.



Li Zhao (S'01) received the B.S.E.E. degree in electrical engineering in 1994 and M.S.E.E. degree in electromagnetic field and microwave technology in 1997 from Nainjing University of Science and Technology, P.R. China. She is now working toward the Ph.D. degree in the Center for Communications and Signal Processing Research, New Jersey Institute of Technology (NJIT), Newark.
 Her research interest is in the area of ultra-wideband (UWB) communications.



Alexander M. Haimovich (M'82–SM'98) received the M.Sc. degree in electrical engineering from Drexel University, Philadelphia, PA, in 1983, the B.Sc. degree in electrical engineering from the Technion, Haifa, Israel, in 1977, and the Ph.D. degree in systems from the University of Pennsylvania, Philadelphia, in 1989.
 He is a Professor of Electrical and Computer Engineering, New Jersey Institute of Technology (NJIT), Newark. He also serves as the Director of the New Jersey Center for Wireless Telecommunications, a state funded consortium consisting of NJIT, Princeton University, Rutgers University, and Stevens Institute of Technology, Hoboken, NJ. His research interests include MIMO systems, array processing for wireless, turbo-coding, space–time coding, and ultra-wideband systems.